Oxidative Addition to Sn(II) Guanidinate Complexes: Precursors to Tin(II) Chalcogenide Nanocrystals.

Ibrahim. Y. Ahmet,[a] [b] Joseph R. Thompson, [a] [b] and Andrew. L. Johnson *[a]

Abstract: SnS, SnSe and SnTe are a potentially important semiconductor materials. Here, we described the application of chalcogen containing Sn(IV) guanidinate precursors, for the production of tin(II) chalcogenide nano-crystals. Reaction of the stannylene (II) guanidinate complex [{$Me_2NC(NCy)_2$}$_2$Sn] (**1**) with Ph_2E_2 (E = S, Se, Te), and CBr_4 forms the Sn(IV) complexes [{$Me_2NC(NCy)_2$}$_2$Sn(Ch-Ph)$_2$] (**2-4**) and [{$Me_2NC(NCy)_2$}$_2$SnBr$_2$] (**5**) respectively. Complex **5** has been subsequently used for the synthesis of the corresponding Sn(IV) mono chalcogenide complexes, [{$Me_2NC(NCy)_2$}$_2$Sn=E] (**6-8**) by the reaction of **5** with Li_2E systems. Isolated tin complexes have characterized by elemental analysis, NMR spectroscopy, and the molecular structures of complexes **2-5** determined by single crystal X-ray diffraction. TG analysis showed complexes **2-4** and **6-8** all to have residual masses close to those expected for the formation of the corresponding 'SnE' systems. Complexes **6-8** were assessed for their utility in the formation of nano-crystalline materials. The materials obtained were characterized by powder X-ray diffraction (XRD), field emission scanning electron microscopy (FE-SEM) and energy dispersive X-ray analysis (EDX). Analysis showed formation of SnSe and SnTe from complexes **7** and **8**, respectively.

Introduction

The family of IV-VI mono-chalcogenide semiconducting materials, and in particular SnS, SnSe and SnTe, have attracted significant attention over the past decade.[1] The mono-chalcogenides 'SnE' (E = S, Se and Te) all display intense absorption across the electromagnetic spectrum, with narrow band gaps (E = S, 1.1 eV (direct), 1.3 eV (indirect); E = Se, 0.9 eV (direct), 1.3 eV (indirect); E = Te, 0.18 eV),[2] and therefore have potential as materials for thermoelectric devices, field effect transistors, superconducting crystals, rechargeable batteries, solar cells and near infrared detectors2015. Significant properties such as charge transfer and charge transport depends strongly on the morphology and crystallinity of the materials i.e. thin films *vs* nanocrystals, size and surface quality.[3]

Over the past two decades research has shown unmistakably, that the most relevant aspect to controlling the morphology of both thin films and nanocrystals is the precise selection of starting molecular precursors,[4] and it is this choice of precursor which determines features such as reaction solvent/temperature, and in the case of nanocrystal/thin film formation deposition/production temperatures.[5]

Lewis *et al.* have recently reviewed routes to both thin film and nanoparticle of IV-VI chalcogenide materials.[1c] A key feature in the development of successful precursors for Sn(II) chalcogenide materials is the ability to control the oxidation state of the tin during the deposition process, so as to suppress the production of materials with variable oxidation states (*i.e.* Sn_2S_3 SnS_2, Sn_2Se_3 and $SnSe_2$) the presence of which can be detrimental to the performance binary Sn(II) chalcogenide materials.[1c, 6] Therefore the ability to control the formation of these materials is paramount and to this end a large number of ligand systems have been developed in an attempt to do so.

As part of an ongoing exploration into the chemistry of group 14 systems and their application in the formation of IV:VI semiconducting materials, such as SnS and SnO,[6-7] we have previously reported the chemistry of the homoleptic Sn(II) guanidinate system [{$Me_2NC(NCy)_2$}$_2$Sn] (**1**). Complex **1**, readily formed in quantitative yields by the insertion of dicyclohexyl-carbodiimide into the {Sn-NMe_2} bonds of [Sn(NMe_2)$_2$] (Scheme 1), has proved to be an intriguing departure point for the synthesis of a range of Sn(IV) guanidinate complexes by reaction with elemental chalcogens (S, Se and Te) as well as single atom chalcogen transfer reagents such as (^{t}Bu)$_3$P=Te,[8] Et_3PSe[9] and styrene sulfide,[10] forming of a range of mono and poly chalcogenide systems of the general form [{$Me_2NC(NCy)_2$}$_2$Sn(E_x)] (E = S or Se; X =1 or 4; Ch = Te, X = 1). While selected tin chalcogen products have found utility in AA-CVD of Sn, SnS, SnSe and SnTe thin films,[11] the product distribution form direct reaction between stannylenes and elemental chalcogens are difficult to control and reaction with single atom transfer reagents, such as Et_3PSe, often results in contamination with phosphine by-products.[7d]

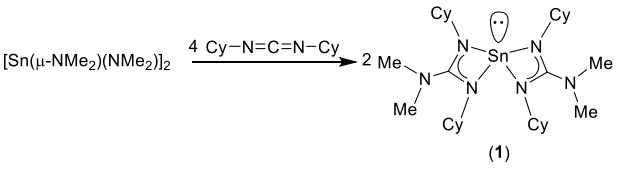

Scheme 1. Synthesis of the homoleptic Sn(II) Guanidinate complexes **1**.

[a] Centre for Sustainable Chemical Technologies
Department of Chemistry,
University of Bath. Claverton Down, Bath, BA2 7AY, UK.

[b] Department of Chemistry,
University of Bath.
Claverton Down,
Bath, BA2 7AY, UK
E-mail: a.l.johnson@bath.ac.uk

Supporting information for this article is given via a link at the end of the document.

In these systems, the unprecedented oxidative control over the resulting thermal decomposition products is such that we have been able to show selective, and exclusive, formation of thin films of Sn, SnS, SnSe and SnTe from an isoreticular series of complexes.

Results and Discussion

Reaction of di-cyclohexylcarbodiimide, in THF, with $Sn(NMe_2)_2$ in 2:1 molar ratio readily affords the homoleptic stannylene complex $[\{Me_2NC(NCy)_2\}_2Sn]$ (**1**). Similar stannylenes have been reported previously.[12] For the purposes of reference, and relevant to our discussion, the molecular structure of complex **1** has been reproduced here and is shown in Figure 1. Complex **1** has previously been fully characterized by solution state NMR (^1H, ^{13}C and ^{119}Sn) spectroscopy and elemental analysis. ^{119}Sn NMR spectra of **1** shows the presence of a single resonance at δ = -380.9 ppm.

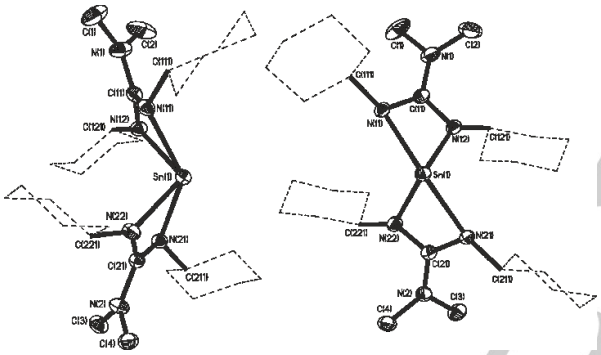

Figure 1. Two views of the molecular structure of the *bis*-guanidinate stannylene complex **1**. Hydrogen atoms have been full omitted, and the cyclohexyl groups have been partially omitted for clarity.

Subsequent reaction of **1** at ambient temperature, with the diphenyl dichalcogenide reagents Ph_2E_2 (E = S, Se and Te) results in the rapid oxidative addition of the {E-E} bond across the stereo-active lone pair of the stannylene, and formation of the Sn(IV) *bis*-phenylchalcogenide complexes, **2-3** as shown in Scheme 2.

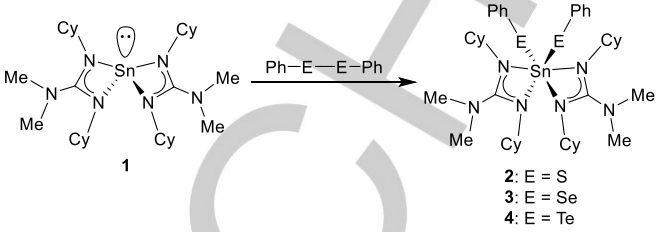

Scheme 2. Synthesis of the Sn(IV) *bis*-Guanidinate *bis*-phenylchalcogenide complexes **2-3**.

Progress of the reaction could be easily followed since a color changes from yellow to colorless (**2**), yellow to orange (**3**) and yellow to red (**4**), respectively were clearly observable. The resulting products were isolated in high yields (63%-89%). ^1H and ^{13}C NMR spectra of the resulting products showed the presence two resonances associated with the {CH} moieties of the *bis*-cyclohexyl guanidinate ligand, indicating a degree of asymmetry in the products. An inspection of the ^1H NMR spectra for 2-4 indicates a 1:1 ratio of the $\{Me_2NC(NCy)_2\}$ ligands and {Ph} groups indicative of the formation of complexes of the general form $[\{Me_2NC(NCy)_2\}_2Sn(E\text{-}Ph)_2]$. This asymmetry is further confirmed with the presence of 12 resonances associated with the {CH} and $\{CH_2\}$ groups on the *bis*-cyclohexyl guanidinate ligand in the 13C NMR spectra for **2**-**4**. ^{119}Sn NMR spectra for complexes **2** and **3** show the presence of single resonances for each of the complexes at δ = -578 ppm (**2**) and -742 ppm (**3**), with additional coupling to the selenium atoms in complex **3** [$^1J_{SnSe}$ = 1410 Hz]. Not unsurprisingly, the ^{77}Se NMR spectrum for **3** shows the presence of singlet resonance [δ_{Se} = 267 ppm] accompanied by satellites generated by coupling to the neighbouring ^{119}Sn centre [$^1J_{SeSn}$ 1411 Hz]. Unfortunately, intensive investigation of compound 4 by 119Sn and ^{125}Te NMR spectroscopy failed to reveal the anticipated Sn and Te resonances.

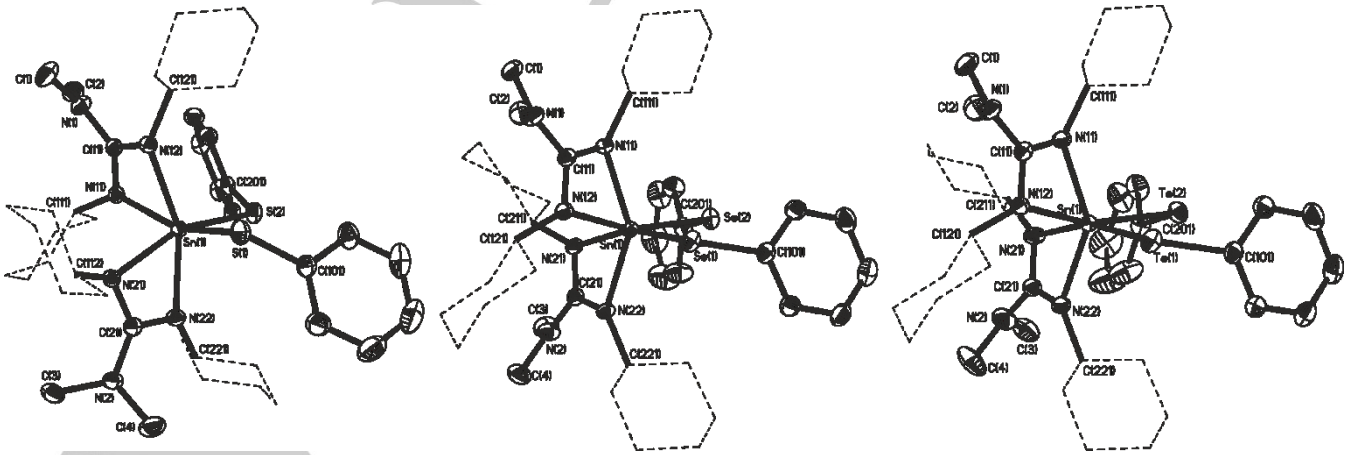

Figure 2. Molecular structure of the Sn(IV) *bis*-phenylchalcogenide complexes **2**-**4**. Hydrogen atoms have been full omitted, and the cyclohexyl groups have been partially omitted for clarity. Disorder in the {Ph} and [13] groups of complex **4** have also been omitted for clarity.

Table 1. Selected bond distances (Å) and angles (°) for **1-4**

	Sn-N	Sn-E	N-Sn-N	E-Sn-E
1[a]	Sn(1)-N(11) 2.4149(12) Sn(1)-N(21) 2.4258(12) Sn(1)-N(12) 2.1780(12) Sn(1)-N(11) 2.1895(12)		N(11)-Sn(1)-N(21) 138.39(4) N(12)-Sn(1)-N(22) 102.54(5) N(11)-Sn(1)-N(22) 96.83(4) N(12)-Sn(1)-N(21) 93.15(4) N(11)-Sn(1)-N(12) 58.03(4) N(21)-Sn(1)-N(22) 57.86(4)	
2[b]	Sn(1)-N(22) 2.1686(12) Sn(1)-N(12) 2.1875(12) Sn(1)-N(11) 2.2307(12) Sn(1)-N(21) 2.2353(12)	Sn(1)-S(2) 2.4859(4) Sn(1)-S(1) 2.5070(4)	N(12)-Sn(1)-N(22) 157.80(5) N(11)-Sn(1)-N(21) 89.33(4) N(11)-Sn(1)-N(22) 107.40(5) N(12)-Sn(1)-N(21) 99.01(4) N(11)-Sn(1)-N(12) 60.78(4) N(21)-Sn(1)-N(22) 60.56(4)	S(1)-Sn(1)-S(2) 95.368(13)
3[b]	Sn(1)-N(11) 2.188(12) Sn(1)-N(22) 2.180(12) Sn(1)-N(12) 2.243(12) Sn(1)-N(21) 2.236(12)	Sn(1)-Se(2) 2.625(4) Sn(1)-Se(1) 2.644(4)	N(11)-Sn(1)-N(22) 146.40(5) N(12)-Sn(1)-N(21) 94.03(4) N(11)-Sn(1)-N(21) 95.92(5) N(12)-Sn(1)-N(21) 95.54(4) N(11)-Sn(1)-N(12) 60.28(4) N(21)-Sn(1)-N(22) 60.52(4)	Se(1)-Sn(1)-Se(2) 94.24(13)
4[b]	Sn(1)-N(11) 2.189(12) Sn(1)-N(22) 2.201(12) Sn(1)-N(12) 2.268(12) Sn(1)-N(21) 2.204(12)	Sn(1)-Te(2) 2.832(4) Sn(1)-Te(1) 2.845(4)	N(11)-Sn(1)-N(22) 143.77(5) N(12)-Sn(1)-N(21) 95.54(4) N(11)-Sn(1)-N(21) 93.86(5) N(12)-Sn(1)-N(21) 94.74(4) N(11)-Sn(1)-N(12) 60.01(4) N(21)-Sn(1)-N(22) 60.40(4)	Te(1)-Sn(1)-Te(2) 95.33(13)

[a] taken from [14]. [b] This work.

Elemental analysis of the complexes similarly suggest the formation of the expected Sn(IV) *bis*-phenylchalcogenide complexes. Single crystals, suitable for X-ray diffraction studies, of complexes **2-3** were obtained upon storage of concentrated hexane solutions at -28 ºC for 12 to 24 hrs. While all three complexes are fundamentally isostructural, complex **2** crystallises in the monoclinic space group $P2_1/n$ with one full molecule in the asymmetric unit, whereas complexes **3** and **4** crystallise in the triclinic space group P-1 again with one molecule per asymmetric unit. The molecular structures for the three complexes are shown in figure 2. Selected bond lengths and angles are provided in table 1.

As noted previously, all three complexes, **2-4**, are isostructural, with analogous gross structural features, i.e. the presence of a central hexa-coordinated *pseudo*-octahedral Sn atom, with the two phenyl chalcodenide groups occupying cisoidal equatorial positions. The remaining four coordination sites are occupied by the nitrogen atoms of the two bi-dentate guanidinate ligands which occupy equatorial and axial coordination site. The differences between the three structures therefore lie in the relative orientation of the phenyl chalcogenide substituents as well as the relative orientation of both the cyclohexyl derivatives and the $\{NMe_2\}$, moieties. Inspection of the complexes reveal Sn-N bond lengths in **2-4** are comparable with related Sn(IV) guanidinate and amidinate complexes in the literature.[10, 15] In all three complexes there is a slight lengthening of the axial and equatorial Sn-N bonds as the atomic number of the chalcogen atom attached the tin centre increases. The significant contraction of the axial Sn-N bonds, in **1**, upon oxidation [ave. ~2.42Å to 2.17-2.19 Å] we presume is due the change in oxidation state of the central tin atom.

Perhaps not unsurprisingly, the average Sn-E bond length increase with the increasing atomic number of the chaclogen atom, and are in good agreement with both comparable Sn-E single bonds within the Cambridge Structural Database (CSD), specifically the related aryl and alkyl-halcogenane compounds such as $[\{(Me_3Si)_2N\}_2Sn(E\text{-}Ph)_2]$[7d] and $[\{(Me_3Si)_2N\}_2Sn(E\text{-}Et)_2]$[16] as well as theoretical values for single bonds calculated from the sum of the single bond covalent radii.[17]

Table 2. Selected distances (Å) and angles (°) for **2-4**

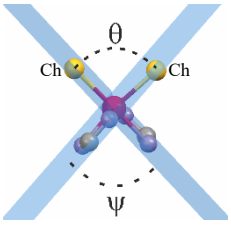

	θ	ψ	[E···E]
2	95.97°	85.65°	3.692 Å
3	94.24°	86.32°	3.861 Å
4	95.32°	85.57°	4.196 Å

Despite the increase in steric demands of the {E-Ph} groups in **2-4** respectively, which is reflected in the lengthening of the Sn-E bonds, there no accompanying change in the {E-Sn-E} angle (θ) or the interplanar {N_2Sn} x {SnN_2} angles (ψ)[15b] (see table 2), (*Cf.* interplanar angles observed in **1** [108.25°]). Although there is a general increase in the [E···E] distance. By the same token, the bite angle of the guanidinate ligands remain similar throughout [**2**: ave. 60.68°, **3**: ave. 60.40°, 4: ave. 60.2°]. One striking feature is the increasing deviation away from linearity of the axial N-Sn-N angle from 157.8° (**2**), to 146.4° (**3**) and 143.8° (**4**), respectively, as the cisoidal chalcogen atoms increase in size.

As part of our study we also wished to investigate an alternative route to the mono-chalcogenide products [{$Me_2NC(NCy)_2$}$_2$Sn=E] (E = S, Se or Te). We have previously described the synthesis of these complexes via the direct reaction of the stannylene **1** with suitable single chalcogen atom transfer reagents. However, we wished to improve the synthetic route by investigating the reactivity of dihalo-Sn(IV) guanidinate complexes with Li_2E (E = S, Se and Te). Reaction of the stannylene **1** with CBr_4 results in the clean oxidation of the Sn(II) center and formation of the di-bromo Sn(IV) complex **5** (Scheme 3). Similar reactivity has been observed with plumbylene systems,[18] although this is, we believe, the first reported example of the reaction of CBr_4 with a stannylene.

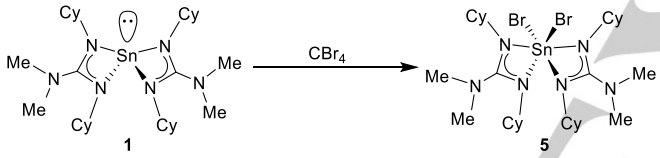

Scheme 3. Synthesis of the Sn(IV) *bis*-Guanidinate *di*-bromo complexes **5**.

Reaction of **1** with equimolar amounts of CBr_4, in THF, results in an immediate color change from pale yellow to red/purple. Removal of the solvent followed by recrystallisation from toluene results in formation of red crystals of **5** in almost quantitative yield (98%). The precise mechanism by which CBr_4 reacts with the stannylene **1** is unknown. However, it is most probable that the mechanism is comparable to similar reactions between stannylenes and alkyl halides,[19] with initial insertion across the Br-C bond, followed by elimination of a putative {CBr_2} fragment. As anticipated, ^{1}H and ^{13}C NMR spectra of complex **5** reveal the presence of resonances associated with both the cyclohexyl {CH} and {NMe_2} groups [^{1}H δ = 3.30 {C(H)}, 3.45 {C(H)} and 2.44 ppm {NMe_2}]. The ^{119}Sn NMR spectrum for **5** shows the presence of a single resonance at δ = -567 ppm, which is comparable to related Sn(IV) di-haogen systems in the literature.[15c] Elemental analysis of **5** closely matched the predicted carbon, nitrogen and hydrogen percentage masses expected for the complex. Figure 3 shows the molecular structure of complex **5**, with selected bond lengths and angles reported in the figure caption. Crystallising in the monoclinic space group *P2$_1$*, complex **5** is a *C$_2$* symmetric dibromo-stannene at the centre of which resides a six-coordinate tin atom with a distorted pseudo octahedral geometry (Br(1), Br(2), N(12) and N(21) atoms in equatorial positions).

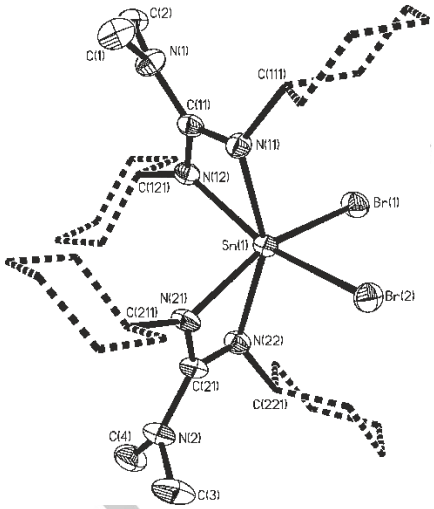

Figure 3. Molecular structure of the Sn(IV) dibromo *bis*-guanidinate complex **5**. Hydrogen atoms have been full omitted, and the cyclohexyl groups have been partially omitted for clarity. Selected bond lengths (Å) and selected bond angles (°): Sn(1)-Br(1) 2.5696(8), Sn(1)-Br(2) 2.5702(9), Sn(1)-N(11) 2.140(6), Sn(1)-N(22) 2.167(5), Sn(1)-N(12) 2.206(6), Sn(1)-N(21) 2.192(6); Br(1)-Sn(1)-Br(2) 92.74(3), N(11)-Sn(1)-N(22) 152.6(2), N(12)-Sn(1)-N(21) 96.7(2), N(11)-Sn(1)-N(12) 61.8(2), N(21)-Sn(1)-N(22) 61.7(2).

The Sn-N bond lengths are again comparable with other Sn(IV) *bis*-guanidinate systems described *ibid*. Similarly, the interatomic Sn-Br distances are comparable to the only other *bis*-guanidinate stannene system containing a Sn-Br interaction reported in the literature.[20] In contrast to the [E-Sn-E] angles in complexes **2-4**, the Br-Sn-Br angle in **5** is notably smaller. Concomitantly, the interplanar {N_2Sn} x {SnN_2} angle [Ψ = 84.3°] only slightly smaller than that observed in complexes **2-4**.

Direct reaction of **5** with either Li_2S, Li_2Se or Li_2Te (made *in-situ* in THF from elemental chalcogens and the super hydride, Li[BEt_3H]),[21] (Scheme 4), resulted in the formation of the corresponding mono-chalcogenide complexes, which after extraction away from THF and LiBr, could be isolated as microcrystalline powders in higher yields [**6**: 81%, **7**: 96%. **8**: 92%] than corresponding reaction between the stannylene **1**, and suitable chalcogenide transfer reagents mentioned previously.[11] The reactions of **5** with the dilithio-chalcogenides resulted in obvious colour changes from a brown/red solution (**5**) to a pale yellow (**6**) and orange solution (**7**), respectively, alongside the formation of a cream coloured suspension.

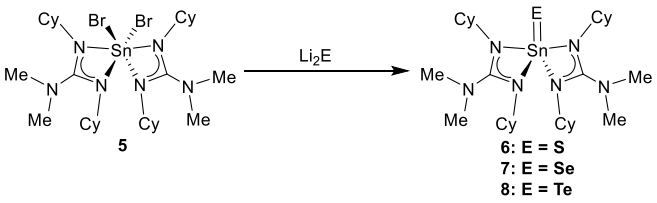

Scheme 4. Salt metathesis synthesis of the Sn(IV) *bis*-Guanidinate mono-chalcogenide complexes **6-8**.

For complex **8**, very little colour change was observed and the reaction was worked-up after a 48hr.

In all cases, characterisation data (^{1}H, ^{13}C and ^{119}Sn NMR spectroscopy and elemental analysis) for complexes **6**-**8** was identical to that previously reported for these complexes.[11]

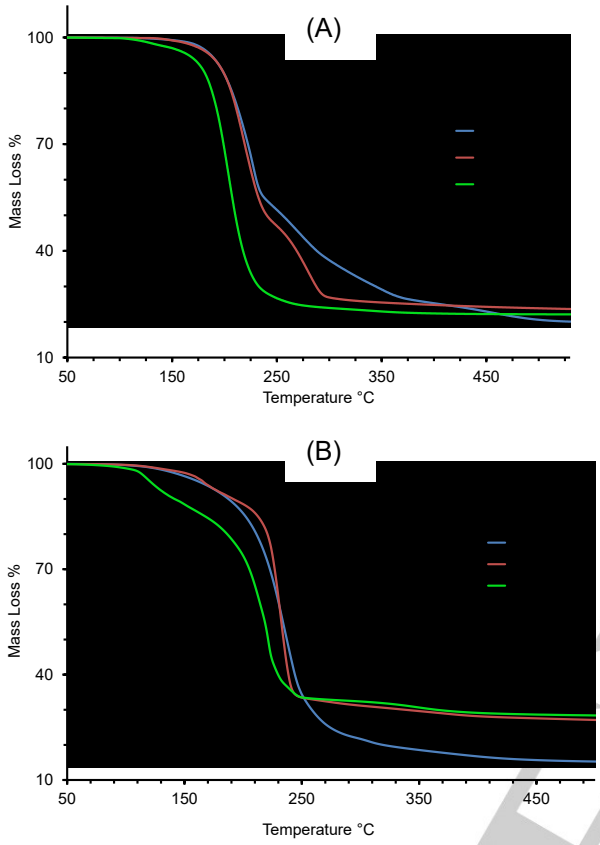

Figure 4. Thermogravimetric analysis data for complexes (**A**) **2**-**4** and (**B**) **6**-**8**.

Thermogravimetric analyses (TGA) of complexes **2-4** and **6-8** were performed in order to gain insight into relative volatilities and thermal stabilities of the compounds (Figure 4). Table 3 gathers relevant data, relating to %-mass residues, expected %-mass residues, onset temperatures and melting points for these complexes. Analyses were carried out with an instrument housed in a nitrogen filled purge-box in order to minimize reaction with atmospheric moisture/air.

Compounds **2-4** (Figure 4A) were found to undergo mass loss to yield stable residues of between 24-25.5 % over the temperature range 289-405 °C. In the case of complex **2** and **3** respectively, the % mass of the non-volatile residues, 25.1% and 25.5%, are both higher than residual masses expected for the formation of the appropriate mono-chalcogenide (i.e. 18.1% for SnS and 21.4% for SnSe). However, It should be noted that the formation of the corresponding di-chalcogenide systems SnS_2 (21.9%) and $SnSe_2$ (29.94%) cannot be ruled out in these systems. In the case of complex 4 the TGA trace reveals a significantly cleaner single decomposition process with a stable %mass residues of 24.2% formed around 348 °C which corresponds directly to the mass residue expected for the formation of SnTe. Contrastingly, the mono-chalcogen derivatives **6**, **7** and **8** all show multi-step decomposition pathways (Fig. 4B) over differing temperature ranges. However, in all three cases the final mass residue is found to be less than that expected, respectively, for "SnS", "SnSe" or "SnTe" formation, possibly indicating a small degree of volatility. It should be noted, however, that the solid state decomposition process monitored in thermogravimetric analysis is probably very different to any solvothermal decomposition process, and can only be used as a general guide.

Table 3: Expected % residue, % of non-volatile residue and onset of volatilisation/decomposition temperature for **2**-**4** and **6**-**8**.

Precursor	Expected % for Residue (Residue)	% Non-volatile Residue (Temp.)	Onset Temp.[§]	Melting point
2	18.1 (SnS) 21.9 (SnS_2)	25.1 (405 °C)	157 °C	133 °C
3	21.4 (SnSe) 29.9 ($SnSe_2$)	25.5 (348 °C)	157 °C	155 °C
4	24.2 (SnTe)	24.2 (289 °C)	124 °C	140 °C
6	23.1 (SnS)	18.6 (349 °C)	121 °C	149 °C
7	28.3 (SnSe)	27.6 (248 °C)	201 °C	115 °C
8	33.2 (SnTe)	28.3 (248 °C)	150 °C	101 °C

Tin Chalcogenide Nanocrystals

In a typical procedure for the preparation of tin chalcogenide nanocrystals, the precursor was dissolved in a minimum volume of hexane. To this solution oleylamine was added and the hexane was removed in vacuo. The reaction mixture was then heated at 210 °C for 40 min before being cooled to room temperature. Excess ethanol was added and the precipitate was collected by ethanol washing and centrifugation three times.

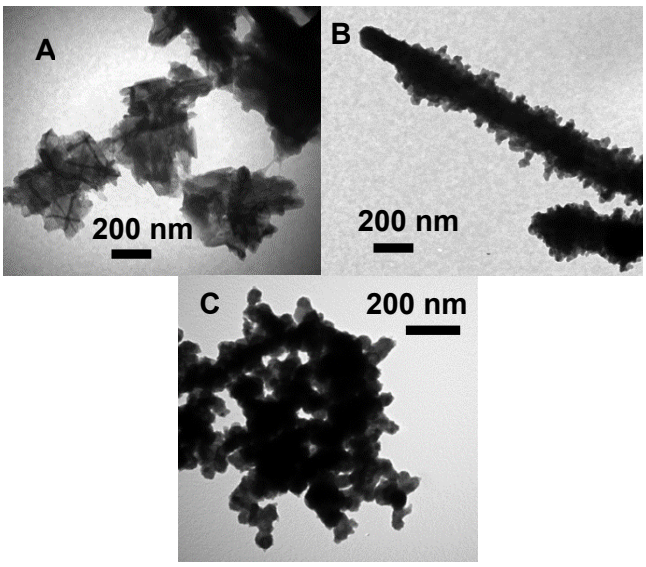

Figure 5. TEM images of nano-crystal synthesised from **A** – **6**, **B** - **7** and **C** - **8**.

The tin chalcogenide precursors **2**–**4** and **6**–**8**, were used in the nanocrystal preparation procedure with varying degrees of success: Compounds **2**-**4** failed to make identifiable chalcogenide containing materials.

While EDX analysis of the materials isolated did show the presence of Sn & S, Sn & Se and Sn & Te respectively, all the materials were Sn rich and contained a high carbon content consistent with an incomplete decomposition and formation of the desired materials. Analysis by PXRD revealed the isolated products to be amorphous.

In contrast, the mono-chalcogen systems **6**-**8** were more successful. After workup, the resulting nanoparticles were analyzed by TEM, the images of the resulting particles are shown in Figure 4. The particles produced over the 40 min reaction time varied considerably in size between ca. 0.4 μm (Figure5 A), 0.5–20-50 nm (Figure5 B) and 50–100 nm (Figure5 C).

EDX spectra for nanocrystals formed from compounds **6**, **7** and **8** respectively all show presence of both Sn and Chalcogen (S Se or Te) in the approx. 1:1 atom-%, Sn/E ratio for materials synthesised over both the 40 min reaction time [Sn:S 49:51; Sn:Se 50:50; Sn:Te 44:56]. It should also be noted that the EDX spectra also showed the presence of trace amounts of Fe, Cu and C, the former arising from the TEM grid used to support the samples (See Supplementary Information).

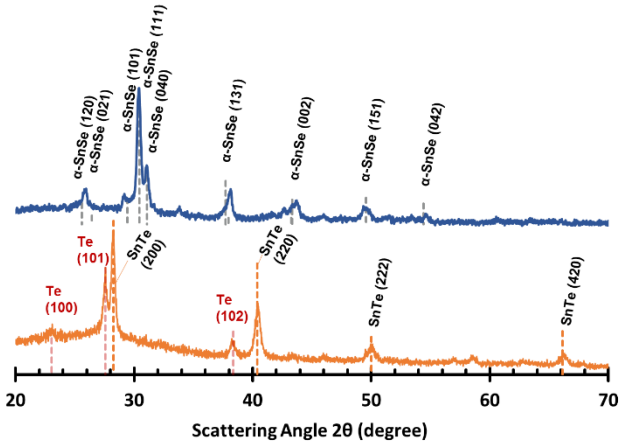

Figure 6. PXRD patterns for (blue) "α-SnSe" and (orange) "SnTe" nanocrystals synthesised from precursors **7** and **8** respectively. NB: * marks the presence of a contaminant within the product.

The materials produced from precursor **6** appear from the TEM images to be thin plate like crystallites. While EDX analysis showed the presence of Sn & S in a ratio of 49:51 and the electron diffraction pattern from the powders was inconclusive showing the presence of only very broad low intensity reflections indicative of small particle size.

For the nanocrystals formed from precursor **7** the TEM analysis shows the crystalline material to have aggregated into stacked plate nano-columns of SnSe similar to SnSe nanocrystals synthesised and reported by K. Jang et al.[22] PXRD analysis of the two materials (Figure 6) confirm the presence of nano-crystals with the PXRD patterns for "SnSe" and "SnTe" matching closely the reported data for the orthorhombic SnSe (Pnma) (JPDS #481224) and cubic SnTe (Fm3m) (JCPDS #652945) respectively.[23] The PXRD pattern of the "SnTe" nano-crystals also shows the presence of a second crystalline component, with peaks at 2θ = 23.06°, 27.60° and 38.30° (Figure 6), which correspond to the existence of hexagonal-Te ($P3_221$) (JCPDS #361452) embedded within the nano-crystalline materials produced.[24]

Conclusions

This work documents the synthesis and characterization of a series of tin(IV) bis-guanidinate complexes **2-4** and **6-9**, and initial investigations into their utility as precursors for the solvothermal synthesis of tin(II) chalcogenide nano-crystals. However, while it should be noted that related complexes have being used in the deposition of thin films of tin(VI) chalcogenides, by spin coating,[25] the work reported here, to the best of our knowledge, represents the first reported use of Sn=E containing systems as single source precursors for SnS, SnSe and SnTe nanoparticle synthesis, with control over the oxidation state of the products. The synthesis for the *bis*-phenyl chalcogenide complexes **2-4** involves the straight forward reaction of the easily prepared stannylene 1, with commercially available diphenyl dichalcogenides Ph_2E_2 (E = S, Se & Te).The molecular structures of all three complex $[\{Me_2NC(NCy)_2\}_2Sn^{[16]}_2]$ (E = S (**2**), Se (**3**) or Te (**4**)) have been determined by single crystal X-ray diffraction experiments, revealing a family of isoreticular complexes, all of which poses a distorted pseudo octahedral geometry about the central Sn(IV) center. As part of our study we wished to access an alternative synthetic pathway to the mono-chalcogen complexes of the general form $[\{Me_2NC(NCy)_2\}_2Sn=E]$ (E = S, Se or Te). To this end, we investigated the reactivity of the stannylene complex **1** with CBr_4, in which the bromoalkane is capable of the oxidative addition of "Br_2" to the Sn(II) centre, resulting in the high yielding formation of the dibromo *bis*-guanidinate complex $[\{Me_2NC(NCy)_2\}_2SnBr_2]$ (**5**), which has been fully structurally characterised. Subsequent reaction of the dibromo species (**5**) with the Li_2S, Li_2Se or Li_2Te respectively results in a new high yielding synthesis of complexes **6**-**8**.

The potential of complexes **2**-**4** and **6**-**8** respectively, as single source precursors for nano-crystal formation (un-optimised) has been evaluated. PXRD and EDX analysis provide clear evidence that under our reaction conditions, the phenyl chalcogenide precursors **2**-**4** fail to form the desired SnE materials, due to incomplete decomposition under our initial reaction conditions. In contrast precursors **6**-**8** all appear (by EDX and PXRD analysis) to produce the desired SnE materials. In the case of precursor **6** PXRD analysis was unable to unequivocally confirm the presence of crystalline SnS. In this case of precursors **7** and **8**, the production of SnSe and SnTe could be confirmed. In the case of precursor **8**, PXRD analysis suggests the possible presence of

additional hexagonal Te to be present in the nano-crystalline product. Our future efforts in this area are directed towards the finding the optimised reaction conditions for the SnE nano-crystal formation, as well as investigating these materials for other thin film and nanomaterial production.

Experimental Section

General Procedures: Elemental analyses were performed using an Exeter Analytical CE 440 analyser. ^{1}H, ^{13}C ^{119}Sn, ^{77}Se and ^{125}Te NMR spectra were recorded on a Bruker Advance 300 or 500 MHz FT–NMR spectrometers, as appropriate, as saturated solutions at room temperature, unless stated otherwise; chemical shifts are in ppm with respect to Me_4Si (^{1}H, ^{13}C). TGA and PXRD were performed using a Perkin Elmer TGA7 or Bruker D8 instrument (Cu-k_α radiation), respectively.

All reactions were carried out under an inert atmosphere using standard Schlenk techniques. Solvents were dried and degassed under an argon atmosphere over activated alumina columns using an Innovative Technology solvent purification system (SPS). The Sn(II) bis-guanidinate, [{$Me_2NC(NCy)_2$}$_2$Sn] (**1**), was prepared by literature method; The reagents Ph_2S_2 Ph_2Se_2 Ph_2Te_2, and CBr_4 were purchased from Aldrich chemicals. Stoichiometric amounts of the dilithio chalcogenides Li_2E (E = S, Se or Te) were synthesized in-situ via using a slightly modified literature method.[21]

Synthesis of [{$Me_2NC(NCy)_2$}$_2$Sn(SPh)$_2$] (2)

Under inert conditions, complex **1** (0.65 g, 1 mmol) and phenyl disulfide (0.23 g, 1 mmol) were dissolved in THF (20 ml). After stirring for 3 hours the solution was dried in vacuo to provide a pale yellow solid. The solid was extracted with hot hexane, and filtered through Celite™. Concentration and storage of the filtrate at -28 °C yielded pale yellow crystals, which were isolated by filtration and dried in vacuo. Yield: 0.56 g, 63 %. ^{1}H NMR (C_6D_6) δ 0.95-2.29 (m, 40 H, Cy-H), 2.39 (s, 12H, N-(CH_3)$_2$), 3.19 (m, 2H, N-C(H)), 3.37 (m, 2H, N-C(H)) 6.92-7.13 (m, 6H, *ortho* and *para-CH*, SC_6H_5), 7.83-7.92 (m, 4H, *meta-CH*, SC_6H_5); ^{13}C {^{1}H} NMR- (C_6D_6) δ 24.56 (Cy-CH), 24.93 (Cy-CH), 25.15 (Cy-CH), 23.41 (Cy-CH), 25.72 (Cy-CH), 25.98 (Cy-CH), 32.68 (Cy-CH), 33.52 (Cy-CH), 33.67 (Cy-CH), 34.10 (Cy-CH), 38.81 (N{CH_3}$_2$), 54.72 (N-CH), 55.82 (N-CH), 124.00 (*para*-CH, SPh), 126.5 (*ortho*-CH, SPh) 135.43 (*meta*-CH, SPh), 138.36 (S-C, SPh) 164.17 (N-C-N); ^{119}Sn {^{1}H} NMR- (C_6D_6) δ -578. Elemental analysis found for $C_{42}H_{66}N_6S_2Sn_1$ (expected): C, 60.21 (60.21); H, 7.98 (7.94), N, 10.02 (10.03); Melting point = 133 °C.

Synthesis of [{$Me_2NC(NCy)_2$}$_2$Sn(SePh)$_2$] (3)

Compound **3** was synthesised under identical conditions to compound 2 using 0.7 g of **1** (1.1 mmol) and 0.35 g of diphenyl diselenide (1.1 mmol).Yield: 0.92 g, 88 %; ^{1}H NMR (C_6D_6) δ 1.16-2.45 (m, 40 H, cyclohexyl), 2.49 (s, 12H, N-(CH_3)$_2$), 3.14 3.19 (m, 2H, N-C(H)), 3.44 3.19 (m, 2H, N-C(H)), 6.94-7.12 (m, 6H, *ortho* and *para-CH*, SeC_6H_5), 7.88-8.05 (m, 4H, *meta-CH*, SeC_6H_5); ^{13}C {^{1}H} NMR- (C_6D_6) δ 26.13 (Cy-CH), 26.41 (Cy-CH), 26.55 (Cy-CH), 26.89 (Cy-CH), 27.19 (Cy-CH), 27.51 (Cy-CH), 33.98 (Cy-CH), 34.95 (Cy-CH), 35.24 (Cy-CH), 36.01 (Cy-CH), 40.27 (N{CH_3}$_2$), 56.12 (N-CH), 57.49 (N-CH), 126.11 (*para*-CH, SePh), 128.19 (*ortho*-CH, SePh) 133.05 (Se-C, SePh), 138.36 (*meta*-CH, SePh) 165.64 (N-C-N); ^{119}Sn {^{1}H} NMR- (C_6D_6) δ -742 (d, $^{1}J_{119Sn\text{-}77Se}$ = 1410 Hz); ^{77}Se {^{1}H} NMR- (C_6D_6) δ 267.12 (d, $^{1}J_{77Se\text{-}119Sn}$ = 1411 Hz) (d, $^{1}J_{77Se\text{-}117Sn}$ = 1344 Hz; Elemental analysis found for $C_{42}H_{66}N_6$ Se_2Sn_1 (expected): C, 54.12 (54.15); H, 7.17 (7.14), N, 9.02 (9.02); Melting point = 155 °C.

Synthesis of [{$Me_2NC(NCy)_2$}$_2$Sn(TePh)$_2$] (4)

Compound **4** was synthesised under identical conditions to compound **2** using 0.8 g of **1** (1.3 mmol) and 0.53 g of diphenyl ditelluride (1.3 mmol).Yield: 0.98 g, 78 %; ^{1}H NMR (C_6D_6) δ 1.10-2.33 (m, 44 H, cyclohexyl), 2.58 (s, 12H, N-(CH_3)$_2$), 6.87-7.34 (m, 10H, N-CH-C_6H_5); ^{13}C {^{1}H} NMR- (C_6D_6) δ 26.23 (Cy-CH), 26.49 (Cy-CH), 26.92 (Cy-CH), 27.04 (Cy-CH), 27.30 (Cy-CH), 27.70 (Cy-CH), 33.89 (Cy-CH), 35.05 (Cy-CH), 35.65 (Cy-CH), 35.83 (Cy-CH), 40.17 (N{CH_3}$_2$), 56.15 (N-CH), 58.18 (N-CH), 113.11 (*para*-CH, TePh), 129.50 (*ortho*-CH, TePh) 137.57 (Te-C, TePh), 143.05 (*meta*-CH, TePh) 165.50 (N-C-N); Elemental analysis found for $C_{42}H_{66}N_6Sn_1Te_2$ (expected): C, 49.01 (49.03); H, 6.46 (6.47), N, 8.16 (8.17); Melting point = Dec. 140 °C.

Synthesis of [{$Me_2NC(NCy)_2$}$_2$SnBr$_2$] (5)

Under inert conditions, complex **1** (0.80 g, 1.3 mmol) and CBr_4 (0.43 g, 1.3 mmol) were dissolved in THF (20 ml). After stirring for 3 hours the solution was dried in vacuo to provide a pale yellow solid. The solid was extracted with 20 ml of toluene, and filtered through Celite™. Concentration and storage of the filtrate at -28 °C yielded red/brown crystals which were isolated by filtration and dried in vacuo. Yield: 0.98 g, 98 %; ^{1}H NMR (C_6D_6) δ 0.77-2.36 (m, 40 H, cyclohexyl), 2.44(s, 12H, N-(CH_3)$_2$), 3.30 (m, 2H, N-C(H)), 3.45 (m, 2H, N-C(H)); ^{13}C {^{1}H} NMR- (C_6D_6) δ 25.76 (Cy-CH), 26.30 (Cy-CH), 26.33 (Cy-CH), 26.69 (Cy-CH), 27.13 (Cy-CH), 27.50 (Cy-CH), 33.48 (Cy-CH), 34.26 (Cy-CH), 35.02 (Cy-CH), 35.88 (Cy-CH), 39.83 (N{CH_3}$_2$), 56.09 (N-CH), 58.30 (N-CH), 165.49 (s, 2C, N=C=N); ^{119}Sn {^{1}H} NMR- (C_6D_6) δ -557; Elemental analysis found for $C_{30}H_{56}Br_2N_6Sn_1$ (expected): C, 46.24 (46.24); H, 7.24 (7.24), N, 10.79 (10.78); Melting point = Dec. 151 °C.

General synthesis of [{$Me_2NC(NCy)_2$}$_2$Sn=Ch] (6 - 8)

Under an inert atmosphere Sulfur (0.06 g, 2 mmol) was suspended in THF (10 ml) of THF. To this solution 4 ml of a 1 M solution of Li[BEt_3H] in THF was added, forming a solution of Li_2S. Complex **5** (1.56 g, 2 mmol) was dissolved in 5 ml THF and added to the Li_2S solution. After stirring overnight the solvents were removed in vacuo and replaced by 10 ml toluene. After filtration from precipitated lithium salts the solvent was removed in vacuo yielding **6** as crystalline residue. Recrystalisation from toluene yielded **6** as pale yellow crystals in approximately 81% yield. (1.05g). ^{1}H NMR (300 MHz, C_6D_6) δ 0.77-2.08 (m, 40 H, Cy-H), 2.69 (s, 12H, NMe_2), 3.44 (m, 2H, NCHC$_5$H$_{10}$), 3.57 (m, 2H, NCHC$_5$H$_{10}$). ^{13}C{^{1}H} NMR- (C_6D_6) 24.87 (Cy-CH) 25.58 (Cy-CH), 25.78 (Cy-CH), 25.85 (Cy-CH), 25.98 (Cy-CH), 26.61 (Cy-CH), 34.93 (Cy-CH), 35.42 (Cy-CH), 36.12 (Cy-CH), 36.60 (Cy-CH), 39.88 (N{CH_3}$_2$), 53.65 (N-CH), 55.74 (N-CH), 165. 39 (N-C-N). ^{119}Sn{^{1}H} NMR (75.8 MHz, C_6D_6) δ_{Sn} -248.0.

For **7**, 0.16 g, 2 mmol of Se was used. Recrystalisation from toluene yielded **7** as orange crystals in approximately 96% yield. (1.34g). ^{1}H NMR (300 MHz, C_6D_6): δ_H 0.99-2.28 (m, 40 H, Cy-H), 2.34 (s, 12H, NMe_2), 3.14 (m, 2H, NCHC$_5$H$_{10}$), 3.36 (m, 2H, NCHC$_5$H$_{10}$); ^{13}C{^{1}H} NMR (75.5 MHz, C_6D_6): δ_c 24.41 (Cy-CH), 24.91 (Cy-CH), 25.00, (Cy-CH), 25.45, (Cy-CH), 25.55 (Cy-CH), 25.92 (Cy-CH), 32.24 (Cy-CH), 32.78 (Cy-CH), 34.77 (Cy-CH), 36.81 (Cy-CH), 38.80 (N(CH_3)$_2$), 54.46 (N-CH), 56.22 (N-CH), 167.7 (N-C-N). ^{119}Sn{^{1}H} NMR (75.8 MHz, C_6D_6): δ_{Sn} -566.3 ^{77}Se{^{1}H} NMR (57.0 MHz, C_6D_6): δ_{Se} -476.01

For **8**, 0.26 g, 2 mmol of Te was used. Recrystalisation from toluene yielded **8** as red crystals in approximately 82% yield. (1.23g) ^{1}H NMR (300 MHz, C_6D_6): δ_H 0.78-2.03 (m, 40 H, Cy), 2.38 (s, 12H, NMe_2), 3.52 (m, 4H, NCHC$_5$H$_{10}$). ^{13}C {^{1}H} NMR (75.5 MHz, C_6D_6): δ_c 26.14 (Cy-CH), 26.95 (Cy-CH), 30.2 (Cy-CH), 39.9 (N(CH_3)$_2$), 56.87 (N-C(H)), 167.33 (N-C-N). ^{119}Sn

{^{1}H} NMR (75.8 MHz, C_6D_6): δ_{Sn} -818 ppm (s); ^{125}Te{^{1}H} NMR (157.98 MHz, C_6D_6): δ_{Te} -1259 ppm.

General preparation of tin chalcogenide nanoparticles from precursors 2-4 and 6-9.

Under inert conditions, excess dry oleylamine (20 ml) was added to a hexane (10 ml) solution of the tin chalcogenide precursor (0.5 mmol). The hexane was removed in vacuo. The reaction mixture was heated at 210 °C for 40 mins (16 also heated for 20 mins and 2 hours). Once cooled to room temperature, excess ethanol was added. The precipitate was collected by centrifugation then purified by ethanol washing and centrifugation a further three times. The powder was dried in vacuo.

Crystallography

Experimental details relating to the single-crystal X-ray crystallographic studies are summarised in the supplementary information (ESI: Table S4). Crystallographic data were collected at 150 K on a Nonius Kappa-CCD Diffractometer [λ($Mo_{k\alpha}$) = 0.71073 Å], and solved by direct methods (SIR-92)[26] and refined against all F^2 using SHELXL–97.[27] All hydrogen atoms are included in idealised positions and refined using the riding model. Structure solution was followed by full-matrix least squares refinement and was performed using the WinGX-1.70 suite of programmes. All non-hydrogen atoms were refined anisotropically. CCDC 1814545 - 1814548 contains the supplementary crystallographic data for this paper. These data can be obtained free of charge at www.ccdc.cam.ac.uk/conts/retrieving.html [or from the Cambridge Crystallographic Data Centre, 12, Union Road, Cambridge CB2 1EZ, UK; fax: +44-1223/336-033; E-mail: deposit@ccdc.cam.ac.uk].

Materials Chemistry

Thermogravimetric analyses (TGA) were obtained using a Perkin Elmer TGA 4000 analyser. Data points were collected every second at a ramp rate of 10 ºC min^{-1} in a flowing (90 mL min^{-1}) N_2 stream.

TEM Images were captured using a Transmission Electron Microscope JEOL 1200 EXII. The TEM was used to capture nm scale images of a range of nano particles and Energy Dispersive X-Ray Spectroscopy (EDS) was captured within the TEM microscope. Data was processed using INCA Wave software. All spectra were standardized and calibrated against a standard copper sample. The magnification, sample level and beam energy (10 keV) were kept consistent between spectral analyses. Nano-powders were dispersed from ethanol suspensions onto carbon coated copper grids and mounted into the TEM. Powder XRD of the nano-powders were performed on a Bruker D8 Powder Diffractometer, using a Cu anode X-ray source, (Kα wavelength = 1.5406 Å) at the University of Bath.

Acknowledgements

We thank EPSRC for funding (EP/L0163541 and EP/G03768X/1) and the Doctoral Training Centre in Sustainable Chemical Technologies (I.Y.A and J.R.T)

Keywords: Tin(II) • Guanidinate • sulphur • selenium • tellurium • Precursors

[1] a) M. Zhou, G. J. Snyder, L. Li, L.-D. Zhao, *Inorg. Chem. Front.,* **2016**, *3*, 1449-1463; b) Z. Wang, P. K. Nayak, J. A. Caraveo-Frescas, H. N. Alshareef, *Adv. Mater.,* **2016**, *28*, 3831-3892; c) D. J. Lewis, P. Kevin, O. Bakr, C. A. Muryn, M. A. Malik, P. O'Brien, *Inorg. Chem. Front.,* **2014**, *1*, 577.

[2] O. Madelung, *Semiconductors: Data Handbook*, Springer, Berlin ; London, **2004**.

[3] a) A. de Kergommeaux, J. Faure-Vincent, A. Pron, R. de Bettignies, B. Malaman, P. Reiss, *J. Am. Chem. Soc.,* **2012**, *134*, 11659-11666; b) Y. Yin, A. P. Alivisatos, *Nature,* **2005**, *437*, 664-670.

[4] a) M. Yarema, R. Caputo, M. V. Kovalenko, *Nanoscale,* **2013**, *5*, 8398; b) D. V. Talapin, J.-S. Lee, M. V. Kovalenko, E. V. Shevchenko, *Chem. Rev.,* **2010**, *110*, 389-458.

[5] P. Marchand, C. J. Carmalt, *Coord. Chem. Rev.,* **2013**, *257*, 3202-3221.

[6] I. Y. Ahmet, M. S. Hill, A. L. Johnson, L. M. Peter, *Chem. Mater.,* **2015**, *27*, 7680-7688.

[7] a) I. Barbul, A. L. Johnson, G. Kociok-Kohn, K. C. Molloy, C. Silvestru, A. L. Sudlow, *Chempluschem,* **2013**, *78*, 866-874; b) T. Wildsmith, M. S. Hill, A. L. Johnson, A. J. Kingsley, K. C. Molloy, *Chem. Commun.,* **2013**, *49*, 8773-8775; c) M. S. Hill, A. L. Johnson, J. P. Lowe, K. C. Molloy, J. D. Parish, T. Wildsmith, A. L. Kingsley, *Dalton Trans.,* **2016**, *45*, 18252-18258; d) J. R. Thompson, I. Y. Ahmet, A. L. Johnson, G. Kociok-Kohn, *Eur. J. Inorg. Chem.,* **2016**, 4711-4720.

[8] T. Tajima, N. Takeda, T. Sasamori, N. Tokitoh, *Organometallics,* **2006**, *25*, 3552-3553.

[9] M. Saito, N. Tokitoh, R. Okazaki, *J. Am. Chem. Soc.,* **1997**, *119*, 11124-11125.

[10] Y. L. Zhou, D. S. Richeson, *J. Am. Chem. Soc.,* **1996**, *118*, 10850-10852.

[11] I. Y. Ahmet, M. S. Hill, P. R. Raithby, A. L. Johnson, *Submitted for Publication,* **2018**.

[12] T. Chlupaty, Z. Padelkova, F. DeProft, R. Willem, A. Ruzicka, *Organometallics,* **2012**, *31*, 2203-2211.

[13] E. Bonnefille, S. Mazières, N. El Hawi, H. Gornitzka, C. Couret, *J. Organomet. Chem.,* **2006**, *691*, 5619-5625.

[14] T. Fjeldberg, H. Hope, M. F. Lappert, P. P. Power, A. J. Thorne, *J. Chem. Soc.,Chem. Comm.,* **1983**, 639-641.

[15] a) Y. L. Zhou, D. S. Richeson, *Inorg. Chem.,* **1997**, *36*, 501-504; b) T. Chlupaty, Z. Ruzickova, M. Horacek, M. Alonso, F. De Proft, H. Kampova, J. Brus, A. Ruzicka, *Organometallics,* **2015**, *34*, 606-615; c) T. Chlupaty, Z. Ruzickova, M. Horacek, J. Merna, M. Alonso, F. De Proft, A. Ruzicka, *Organometallics,* **2015**, *34*, 2202-2211.

[16] G. Bendt, S. Lapsien, P. Steiniger, D. Bläser, C. Wölper, S. Schulz, *Z. Anorg. Allg. Chem.,* **2015**, *641*, 797-802.

[17] L. Pauling, *"The Nature of the Chemical Bond". Third edition*, Cornell University Press, Ithaca, N.Y., **1960**.

[18] N. Kano, N. Tokitoh, R. Okazaki, *Organometallics.* **1997**, *16*, 2748-2750.

[19] Z. Padělková, P. Švec, V. Pejchal, A. Růžička, *Dalton Trans.,* **2013**, *42*, 7660.

[20] T. Chlupatý, Z. Růžičková, M. Horáček, J. Merna, M. Alonso, F. De Proft, A. Růžička, *Organometallics,* **2015**, *34*, 2202-2211.

[21] H. Lange, U. Herzog, U. Böhme, G. Rheinwald, *J. Organomet. Chem.* **2002**, *660*, 43-49.

[22] K. Jang, I. Y. Lee, J. Xu, J. Choi, J. Jin, J. H. Park, H. J. Kim, G. H. Kim, S. U. Son, *Cryst. Growth Des.,* **2012**, *12*, 3388-3391.

[23] H. S. Im, Y. Myung, Y. J. Cho, C. H. Kim, H. S. Kim, S. H. Back, C. S. Jung, D. M. Jang, Y. R. Lim, J. Park, J. P. Ahn, *RSC Adv.,* **2013**, *3*, 10349-10354.

[24] Z. L. Li, S. Q. Zheng, Y. Z. Zhang, R. Y. Teng, T. Huang, C. F. Chen, G. W. Lu, *J. Mater. Chem. A,* **2013**, *1*, 15046-15052.

[25] M. Bouška, L. Střižík, L. Dostál, A. Růžička, A. Lyčka, L. Beneš, M. Vlček, J. Přikryl, P. Knotek, T. Wágner, R. Jambor, *Chem. Eur. J.,* **2013**, *19*, 1877-1881.

[26] A. Altomare, G. Cascarano, C. Giacovazzo, A. Guagliardi, M. C. Burla, G. Polidori, M. Camalli, *J. Appl. Cryst.,* **1994**, *27*, 435-436..

[27] G. M. Sheldrick, *Acta Crystallogr. A,* **2008**, *64*, 112-122.

Entry for the Table of Contents

FULL PAPER

SnS, SnSe and SnTe are a potentially important semiconductor materials. Here, we have described the application of mono chalcogen Sn(IV) guanidinate precursors, containing either Sn-Ch or Sn=Ch bonds (Ch = S, Se and Te) derived from the oxidative addition of elemental chalcogenides (S, Se and Te) and Diphenyl dichalogenides to Sn(II) guanidinate complexes, for the production of tin(II) chalcogenide nano-crystals.

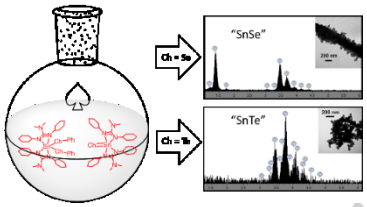

Key Topic* Nanocrystal Precursors, Tin(II) Chalcogenides

*I. Y. Ahmet,[a] [b] Joseph R. Thompson, [a] [b] and A. L. Johnson **

Page No. – Page No.
Oxidative Addition to Sn(II) Guanidinate Complexes: Nanocrystal Precursors.